XXXVI Ibero-Latin American Congress on Computational Methods in Engineering
CILAMCE
Rio de Janeiro, 22-25 Nov 2015

NONLINEAR FINITE ELEMENT MODELING OF THE WIRE DRAWING PROCESS OF STEEL INCLUDING FRICTION

[1]**Mirela Oliveira de Castro**

mirela.castro@alu.ufc.br

Universidade Federal do Ceará

Campus do Pici, s/n. Bloco 729, 60440-554, Fortaleza-CE, Brazil.

[2]**Péter Zoltán Berke**

pberke@ulb.ac.be

Abstract. *Wire drawing is commonly used in industry, mainly for the mass fabrication of wires and rods. It couples production efficiency with good superficial quality of the final product and it provides an increase of the material strength through the plastic straining during the metal forming. The numerical work presented here focuses on the finite element simulation of the wire drawing procedure. The main motivations of the work are a deeper understanding of the wire drawing procedure and the future prediction of the wire drawing parameters and product quality as a function of the material properties of the raw material. A pre-existing nonlinear model, using the finite element method, was adapted to the wire drawing process, identifying the dominating parameters. The developed model includes the following nonlinear ingredients: contact/friction treatment through the augmented Lagrangian method, corotational finite strain formulation, elastic-(visco)plastic material behavior with isotropic nonlinear hardening. It uses an axisymmetric modeling assumption, considering the cylindrical shape of the work piece. This model allows for observing in details the phenomena occurring during the wire drawing and it is used for a computational investigation of the wire drawing parameters (friction between die and work piece, die semi-angle, material properties, etc) and their influences.*

Keywords: *Nonlinear finite element, wire drawing, friction, (visco)plasticity.*

[1] Metallurgical Engineering undergraduate student - Universidade Federal do Ceará (UFC)
[2] Visiting professor - Universidade Federal do Ceará (UFC)

1 INTRODUCTION

Among the mechanical forming processes commonly used on metals the drawing process stands out by performing in a simple and economical way the production of rods, bars and wires with various diameters (even smaller than a millimeter). It is a widely used process in the rod fabrication for civil engineering, wires for welding electrode etc. The process consists in reducing the diameter of a wire passing it through the hole of the die and, as a by-product, changing its mechanical properties by cold plastic deformation suffered by the material. The die has a conical shape on its front, where the wire enters to continuously reduce the cross section of the wire to the desired diameter. In the center of the die there is a cylindrical area with a function to stabilize the new dimensions of the wire. The rear part of the tool, corresponding to the wire outlet area, has a conical shape to gently release contact between die and wire. Fig. 1 shows schematically the process of reduction of the wire cross-section in a sectional view at. The angle α, as shown in Fig. 1, represents the die inlet semi-angle, L is the length of the cylindrical region in the center of the tool, D_0 and D_f represent the initial and final diameters, respectively. The section reduction range for steel, per wire drawing pass, is between 10 and 30%, while its reduction over 8 to 15 passes can reach 95% (Cunningham, 2008).

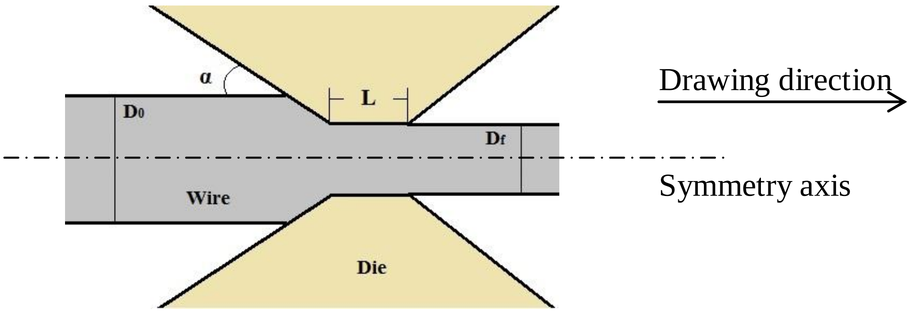

Figure 1. Scheme of the studied wire/die system.

According to Chin and Steif, (1995), the drawing process has been studied since at least 1927. Much has already been discovered about it, as parameters that define the inlet angle suitable for drawing at high speeds (Cristecu, 1980), the wire fracture prediction by elastic-plastic model (Chevalier, 1992), and the inhomogeneity of the strains caused by drawing (Chin and Steif, 1995). Currently, several research efforts focus on process optimization through parametric studies, such as the evolution of defects during the drawing (Baek et al, 2012), causes and effects of increased process temperature (Toribio et al (2014) and El - Domiaty and Kassab (1998)), the effects of strain rate on the material properties during the process (Huh et al, 2013), defect types shown on the material before and after reduction (Magalhães et al, 2012), study tool wear (Kim et al, 1997), and others.

Within this context, the computational analysis has contributed substantially to a deeper understanding of drawing as it allows us to observe in details the phenomena occurring during the process from a different perspective than experimental works. Is possible to check with a good approximation of real life process how material and tool behave during the reduction of the cross section.

El-Domiaty and Kassab (1998) performed a parametric study analyzing the influence of friction, die semi-angle, drawing speed and rate of reduction in the tool outlet temperature for ten different materials, through an analytical model. This was validated with low error by experiments. Haddi et al (2011) conducted experiments to analyze the effects of process conditions on temperature and drawing strength in a copper alloy. The results showed an increase in the temperature due to friction (lubricating contact conditions); a peak temperature in the region close to the tool/workpiece interface, due to the greater plastic deformation and; the dependence of the distribution of stresses in the material according to the wire drawing speeds.

Chin and Steif (1994) studied by computational modeling, the inhomogeneity of plastic deformation in a single pass drawing and their impact on drawing force, concluding that the mechanical redundant (excessive and undesirable) work is a function of the area reduction and the tool entry angle; and that friction between the tool and wire and work hardening do not significantly influence the deformation. Celentano et al (2009) constructed a finite element model for a drawing process with 12 passes, at low drawing speeds (between 1 and 80 mm/min), confirming that relatively simple models can, illustratively, describe the behavior of the material response under complex deformation conditions. Bihamta et al (2011) proposed a new model for drawing aluminum tubes by combining the models without mandrel and fixed mandrel to obtain thickness variation of the tubes in the axial direction. The model was tested numerically and experimentally validated.

Baek et al (2012) observed the development of surface defects of various shapes on drawn wires through 3D simulations comparing computational results with experimental results obtained from medium carbon steel samples with rounded defects as a function of drawing strain. It was noticed that the final shape of the imperfections is determined according to the distribution of radial and circumferential stresses. Felder et al (2012) studied a new way to calculate the stresses caused by friction, without requiring prior knowledge of the characteristic stress-strain curve of the material, through a thermomechanical computational model having as main parameters the drawing force and the temperature. This research showed that there is a linear relationship between the force and the drawing process temperature to different coefficients of friction.

A computational parametric study by Filice et al (2013) for copper drawing, analyzes drawing force, tool wear, damage and thinning by varying the inlet die semi-angle and the deformation suffered by the material (D_0/D_f) in order to optimize the process. This concluded that the optimum parameters for the process can be calculated based on the key parameter (drawing force), which depends on the requirement of process analyst. Toribio et al (2015) presents an innovative model of die geometry with two inlet angles to reduce residual stresses and improve the material's resistance to hydrogen embrittlement. A numerical model was constructed to compare the distribution of residual stresses and deformation between the conventional and the new geometry. From the results, it was understood that the reduction of the residual stresses mainly depends on the angle used for the second reduction, which should be as small as possible.

There is a significant body of literature dedicated to the drawing process, although much remains to be understood about it. Coupled physical phenomena and parametric relationships in the drawing need more detailed analysis, since the process has a simple principle but complex mechanics. This paper aims to contribute to the state of the art on wire drawing.

The focus of this paper is the development and use of a finite element model for drawing. This motivated by the ability to observe, in detail, how the stresses and deformations are distributed in the material during and after reduction (product). It is thus possible better understand the phenomenon of inhomogeneity of deformation and non-compliance linearity in the mechanical behavior of the wire. The study aims to show how the angle of drawing, the yield strength, friction and the drawing speed influence the distribution of stresses and strains in the material through computer simulation.

The numerical model is described below, as well as information about the mesh and the behavior model of the reference material are given. The simulation results are presented in Section 3, followed by a comparative study of the various tested conditions, a brief discussion and succinct conclusion.

2 THE DEVELOPED NUMERICAL SINGLE PASS DRAWING MODEL

To simulate the process of drawing, a finite element program in MATLAB language was adapted for this study. The entire process is represented as axisymmetric, i.e. only a planar section of the system is used for the computations. This choice reduces the central processing unit (CPU) time because of solving for less degrees of freedom in the simulations. In this model the tool is considered as a rigid body and the wire as a deformable body, justified by the high hardness of the die material compared to the wire.

The wire has 5.5 mm in diameter and 8 mm in length, sufficient to analyze the process without observing edge effects when using as maximum displacement 7 mm. This choice is due to the need to reduce the computing time by using less variables to discretize a smaller body. The wire leading end has a diameter 5mm, representing the region where drawing force is applied to the wire passing through the die and corresponding to a 10% reduction of the wire diameter. The die has a drawing angle α of 5º, 7º and 9º in the parametric study, close to those used in industrial processes (Toribio et al, 2014). The tool also has a length of the cylindrical region of about 1 mm (length L in Fig. 1).

In addition to the three above-mentioned drawing angles, some of the process and material parameters were also varied in order to study their effects. It is known that the geometry of the tool has significant influence on drawing strength and homogeneity of deformation along the wire radius (Toribio et al, 2014). Furthermore, the coefficient of friction is another parameter that influences the drawing force and is a dominant factor in tool wear, leading to breakage of the wire (Filice et al, 2013). The initial yield strength of the material is an important parameter in the study of forming processes, since this parameter represents a limit of the nonlinear behavior of metallic materials.

2.1 The constructed FE mesh

The wire mesh was verified to be converged, i.e. it has similar results to simulations with finer mesh. It has 1348 elements and 8394 degrees of freedom for a piece of eight millimeters length and 2.75 millimeters of initial radius. The mesh was created in GMSH program using a parameterized file. The elements are of quadrilateral with eight nodes per element, in a corotational finite strain fomulation (natural decoupling of the rigid body rotation and deformation (Ponthot, 2002)). The contact conditions for the tool/wire system are handled by the augmented Lagrangian method (Pietrzak and Curnier, 1999 and Heegaard and Curnier, 1993). The computer time for every quasi static simulation was, on average, 5 hours, and for the simulations with 4 m/s drawing speed was about 3 hours. This long computational time is due to a high mesh refinement and to the treatment of all the nonlinearities involved.

Fig. 2 shows (a) the boundary conditions and the used FE mesh and the internal tool contours, according to the drawing angle α presented in zoom for better viewing (b).

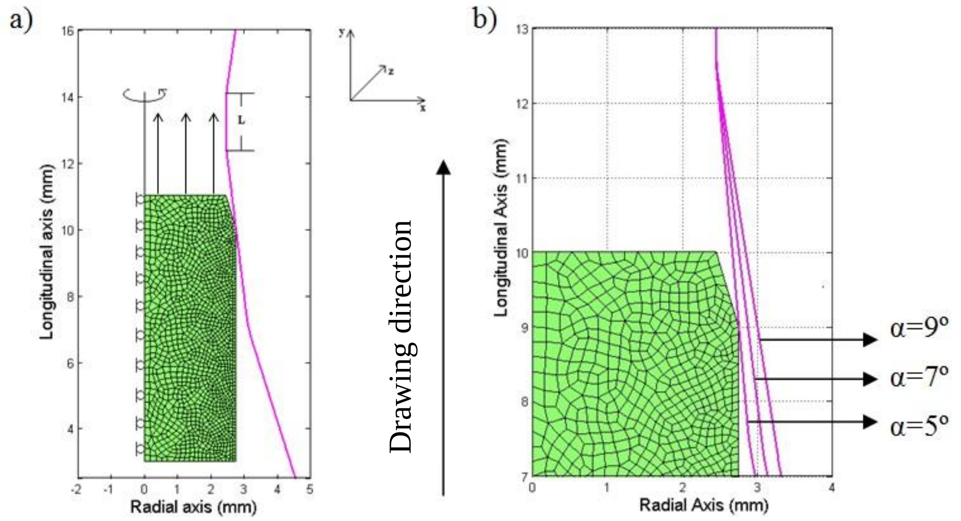

Figure 2. (a) Boundary conditions, FE mesh and rigid die with (b) the three studied drawing angles.

2.2 Material model

The material studied in this article is a low carbon steel, commonly used in metalworking industries to make rebars for reinforced concrete structures for civil engineering applications. An isotropic material with nonlinear hardening elastic-plastic (independent of strain rates) and elastic-viscoplastic (dependent on the strain rates) behaviors was considered. Eq. (1) corresponds to the yield function of the material. This function returns negative values in the elastic range, i.e., the von Mises stress, σ_{eq}, is less than the current yield stress, σ_y. Positive values trigger their (visco)plastic behavior of the material. Equation (2) shows the evolution of the yield strength of the material as a function of accumulated plastic strain, κ, and its $\dot{\kappa}$ rate (time-dependent). σ_0 corresponds to the initial yield strength (for $\kappa = 0$), while the second term of Eq. (2) describes the non-linear hardening behavior (for $n \neq 0$ and $n \neq 1$). The third term is active for $\eta \neq 0$ and represents the overstress due to the dependence on the plastic strain rate. Increasing the value of $\dot{\kappa}$ the overstress also increases, following the model of Perzyna (Jorge, 2005).

$$f(\sigma, \kappa, \dot{\kappa}) = \sigma_{eq}(\sigma) - \sigma_y(\kappa, \dot{\kappa}) \quad (1)$$

$$\sigma_y(\kappa, \dot{\kappa}) = \sigma_0 + K\kappa^n + \sigma_0\eta\,\dot{\kappa}^{nvp}. \quad (2)$$

In the above equations, and this work, σ and κ correspond respectively to stresses in the material and the scalar measure of plastic deformation of the material. The material parameters used in the model are: the modulus of elasticity (E = 208 GPa), Poisson's ratio (ν = 0.3), the strain hardening exponent (n = 0.6), the work hardening coefficient (K = 515,23 MPa), the initial yield strength (σ_0 = 275 MPa), the viscoplasticity coefficient (η) and the exponent of viscoplasticity (n_{vp}). The η value is nonzero only for viscoplastic simulations. The value of 0.01 was adopted for this parameter in order to provide an apparent yield strength of approximately twice for strain rates close to the ones observed in simulations for 4 m/s, compared to the quasi-static computations. n_{vp} was kept equal to 1 in all simulations to maintain the linearity of the third term of Eq. (2) function and a simplified computation. Fig. 3 illustrates the force vs. displacement curves for the used material model at different strain rates in a compression test.

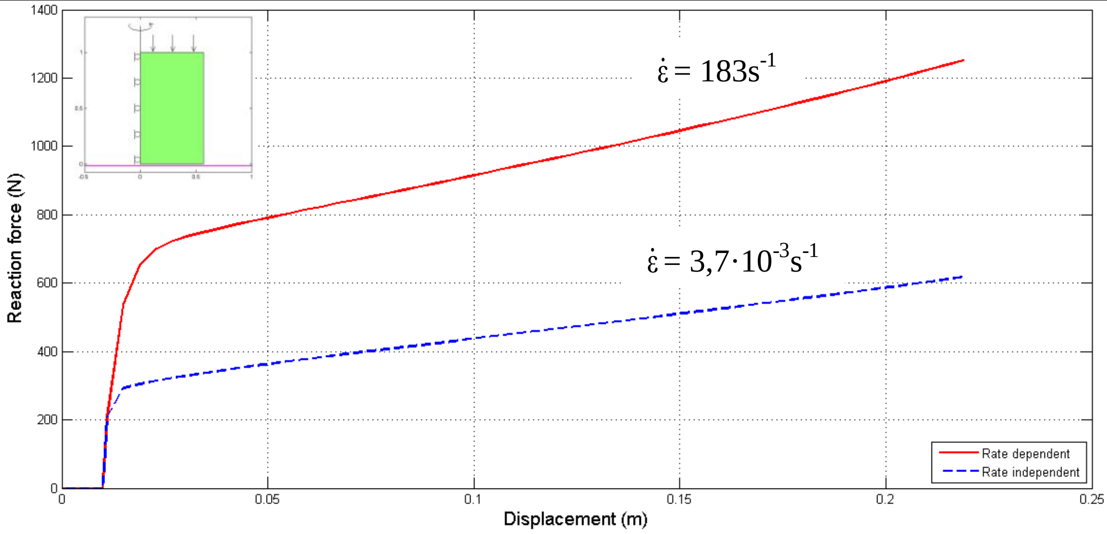

Figure 3. Behavior of the viscoplastic material model in simulated compression tests.

The friction coefficient μ was used according to Coulomb's law and V is the drawing speed, chosen to correspond to values used in the industry (Haddi et al, 2011). Table 1 shows combinations of parameters used for each simulation.

Tabela 1. Parameters of the performed simulations

Simulação nº	Ângulo α (º)	σ_0 (MPa)	μ	η	V (m/s)
1	5	275	0,1	0	~ 0
2	5	275	0	0	~ 0
3	5	330	0,1	0	~ 0
4	5	330	0	0	~ 0
5	5	275	0,1	0,01	4
6	5	275	0	0,01	4
7	7	275	0,1	0	~ 0
8	7	275	0	0	~ 0
9	9	275	0,1	0	~ 0
10	9	275	0	0	~ 0
11	9	275	0,1	0,01	4
12	9	275	0	0,01	4

3 NUMERICAL RESULTS AND DISCUSSION

The results of the quasi-static drawing simulations are presented below, followed by results at 4 m/s in Section 3.2. The first simulation listed in Table 1 was used as the reference case for the parametric comparative study, and is presented first.

3.1 Quasi static drawing

REFERENCE CASE

The simulation with α=5º, initial yield strength of 275MPa, friction coefficient of 0,1 and drawing speed $V=1\cdot10^{-5}$m/s was chosen as the reference case.

Figure 4 presents the results for the stresses in the radial, longitudinal, circumferential directions as well as the in-plane shear and von Mises equivalent stress. The line separating zones 1 and 2 in Fig. 4 (a) marks the domains of material forming (contact between tool and workpiece) and product (residual stresses), respectively, in all figures.

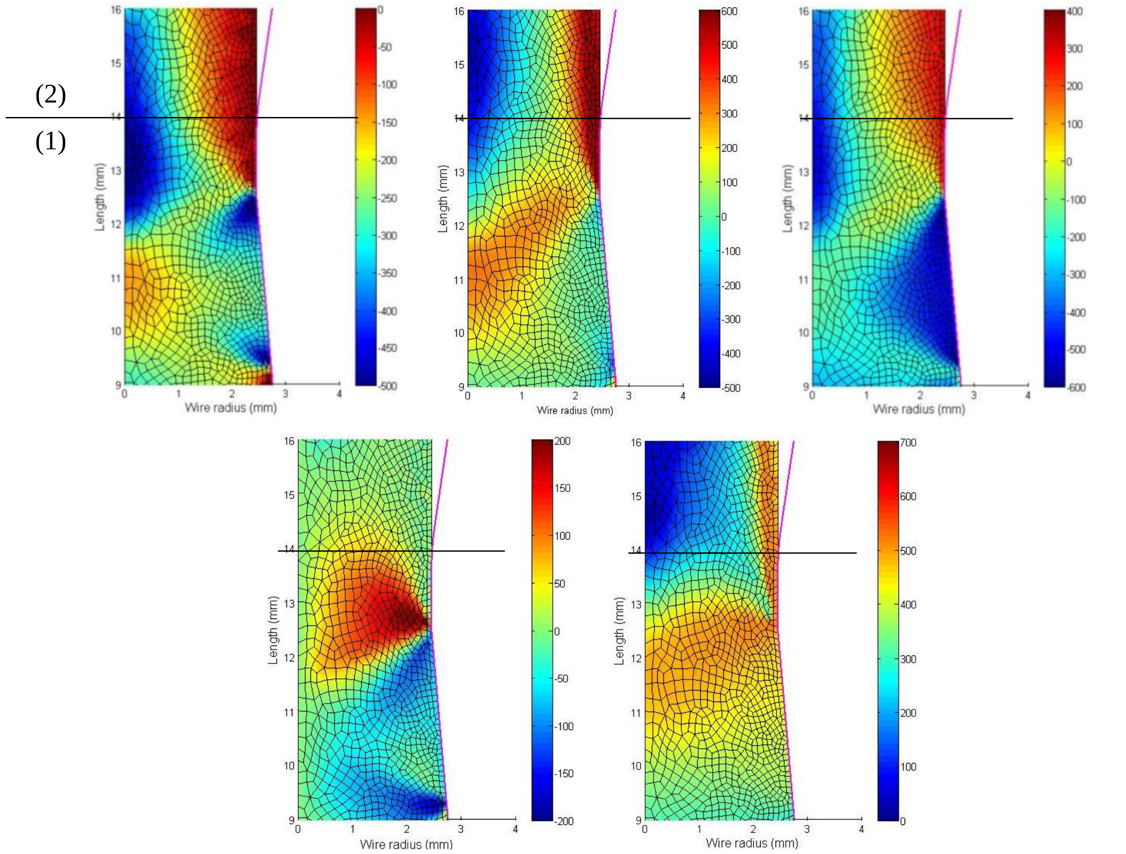

Figure 4. Distribution of the stresses in MPa, along the (a) radial (b) longitudinal and (c) circumferential axes, (d) in-plane shear and (e) von Mises equivalent stress at 7 mm drawing displacement.

The compressive radial stresses in the forming zone predominate due to the thickness reduction in this direction, and are the highest on the wire surface at the beginning of the contact with the tool and at the narrowest part of the cone of entry. There are also compressive stresses in the center of the wire as it exits the conical region of the inlet and passes to the cylindrical region of the tool. In the circumferential direction compressive stresses of about 500MPa are formed throughout the region of the inlet cone due to circumferential compression caused by the reduction of cross section

Tensile stresses predominate in the longitudinal axis. They are higher in the center of the wire during the conical reduction and intensified on the surface of the wire as it passes into the cylindrical region of the tool. Shear stresses show concentration points at the beginning of the contact with the tool and at the end of the inlet cone. They gradually reach lower values in the central region of the wire. The von Mises stress is relatively uniform along the conical zone 1 and reaches a maximum of about 500MPa.

The radial residual stresses (zone 2) are essentially compressive and they decrease to values close to zero in the center to edge direction of the wire. In the longitudinal axis residual compressive stresses are formed at the center of the wire, decreasing gradually to give way to tensile stresses that reach 600MPa on the surface. A similar distribution is observed in the circumferential direction, although the variation is smaller (between -400 and 300MPa) than along the longitudinal axis (between -400 and 600MPa). Residual shear stresses were not observed. A narrow shell just below the surface of the wire, concentrates the highest von Mises stresses (approximately 550MPa), meaning that an additional deformation would take place more easily in this layer near the surface.

Figure 5 shows the total deformations in the radial, longitudinal and circumferential directions and shear, and also the scalar plastic deformation measure (κ) and its rate ($\dot{\kappa}$).

In both radial and longitudinal directions, the deformation of the product is homogeneous throughout the wire diameter reaching a maximum of 12% in compression along the circumferential direction, 10% (as expected) in the radial and 23% of traction along the axial directions. The plastic deformation was approximately 30% at a very small rate ($\dot{\kappa}$), due to the assumed quasi-static drawing.

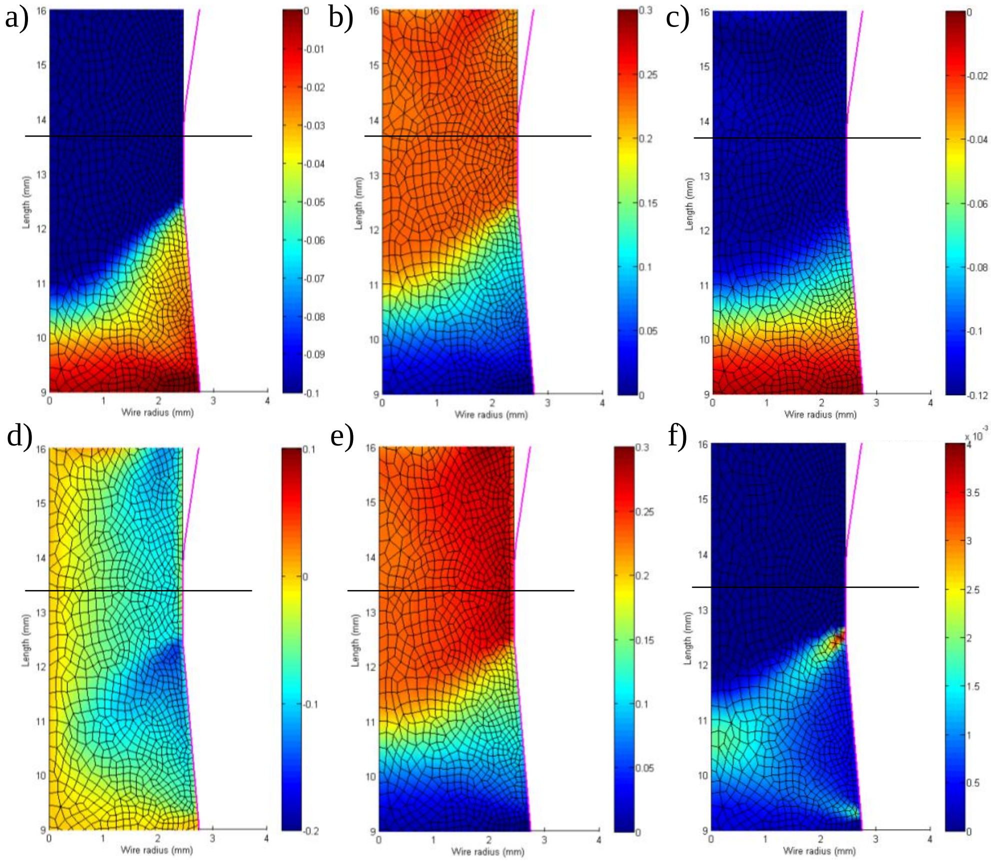

Figure 5. Deformation along the (a) radial, (b) longitudinal and (c) circumferential directions, (d) shearing, (e) scalar plastic deformation measure (κ) and (f) rate of scalar plastic deformation measure ($\dot{\kappa}$) for a drawing displacement 7mm.

The next three topics present the results of quasi static simulations. First the influence of yield strength on the results is shown, followed by the effect of varying the inlet α angle and finally by the variation of friction in the process.

INITIAL YIELD STRENGTH

In Fig. 6 are shown the force x displacement curves for tests carried out with an initial yield strength of 330MPa and 275MPa.

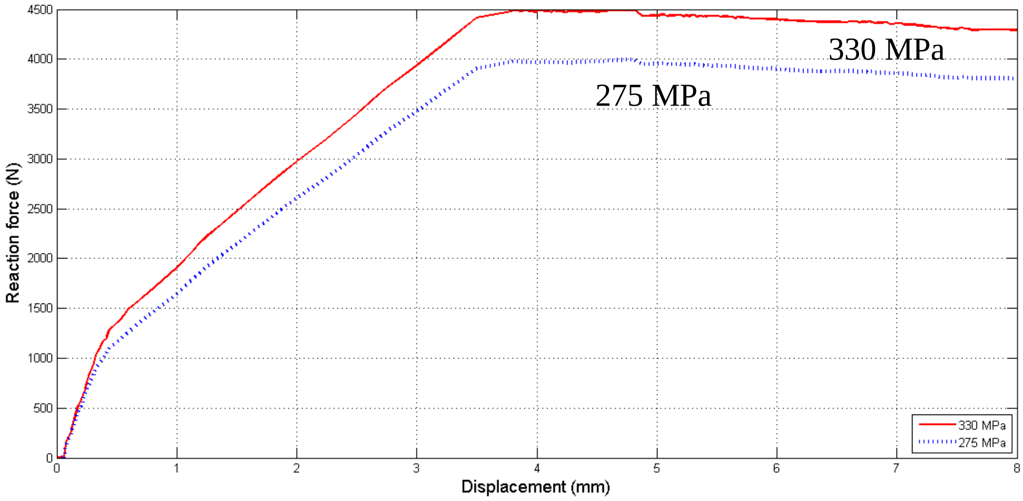

Figure 6. Force x displacement curves for different initial yield strengths.

The behavior of the material with a 20% increase in its initial yield strength (other parameters remain unchanged) presented a maximum drawing force of about 12.5% higher. This indicates that this parameter is a factor of direct influence on the drawing force. Note that this variation of 20% in the yield strength can be considered mild from the industrial point of view.

DIE INLET ANGLE

Fig. 7 shows the distribution of von Mises stress in the wire for inlet angles of 5º (a), 7º (b) and 9º (c), keeping the other parameters equal to the reference case.

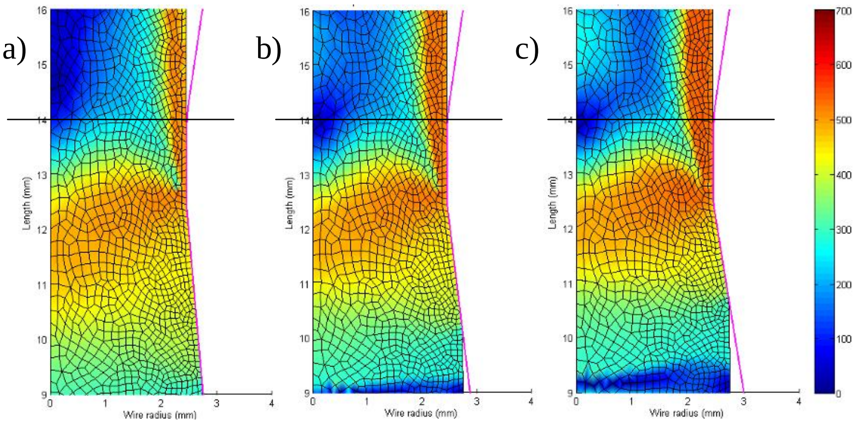

Figure 7. Distribution of von Mises stress (MPa) for 5º, 7º and 9º die inlet angle a), b) and c), respectively.

For the simulations with α equal to 7º and 9º, a higher inhomogeneity of the residual stresses can be observed. The high stress layer (orange region in the product zone) is thicker than for 5º. The increase of α implies smaller contact zones in which the material is formed (Fig.7). This results in higher stress and strain gradients in the forming zone. The fact that the forming operation is performed on a smaller tool surface possibly leads to higher tool wear as well.

This also has implications on the frictional behavior, since obviously the contact geometry and response are naturally coupled.

FRICTION

Fig. 8 shows the force x displacement curves as a result of the test performed with α equal to 5º, 7º and 9º, σ_0 equal to 275MPa, with and without friction.

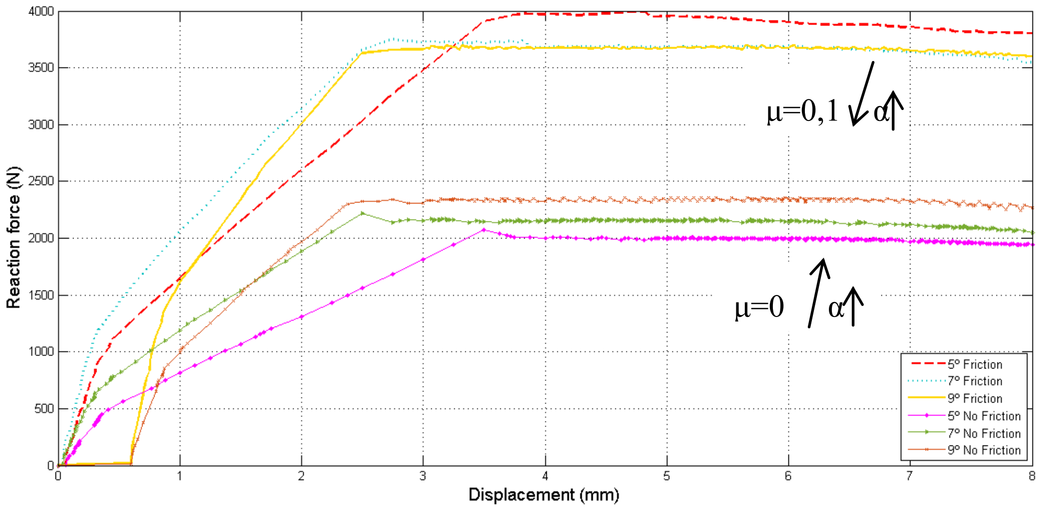

Figure 8. Curves Force x Displacement of the material resulting from the tests with and without friction, for angles 5º, 7º and 9º and initial yield strength 275MPa.

The simulations with and without friction shown that the deformations undergone by the wire are enhanced by friction, keeping relatively similar stress distributions as in the frictionless case.

Fig. 8 shows the large increase in the required drawing force when friction is considered, compared to the frictionless case. When no friction is taken into account, increasing α lead to increasing drawing forces, as expected. In the case of μ=0,1this trend seems inversed.

The main difference in the total strain distribution was observed in shear when considering friction, as expected in Fig. 9.

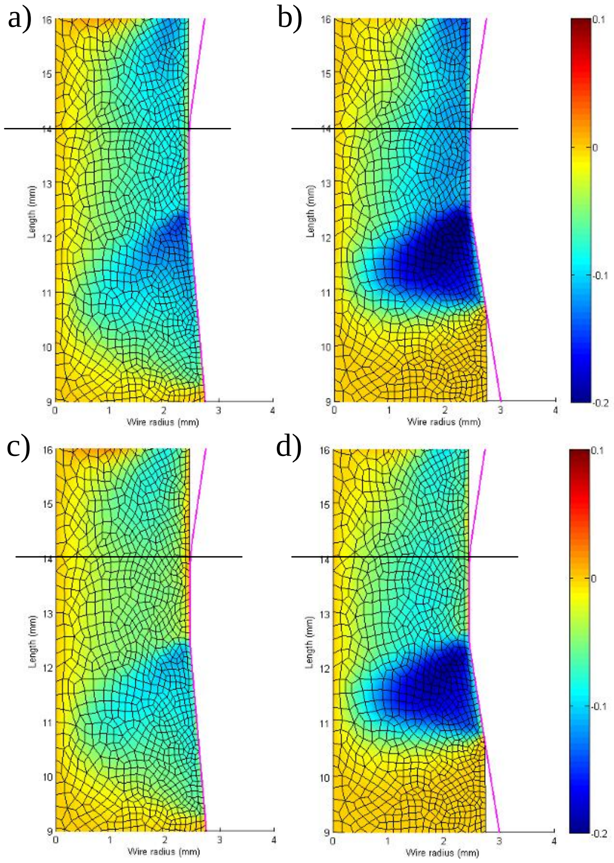

Figure 9. In-plane shear deformations a) α=5º and μ=0,1, b) α=9º and μ=0,1, c) α=5º and μ=0 and d) α=9º and μ=0.

3.2 Simulations with rate dependent plastic behavior

The behavior of metallic materials exhibits a strain rate dependence (Fig. 10).

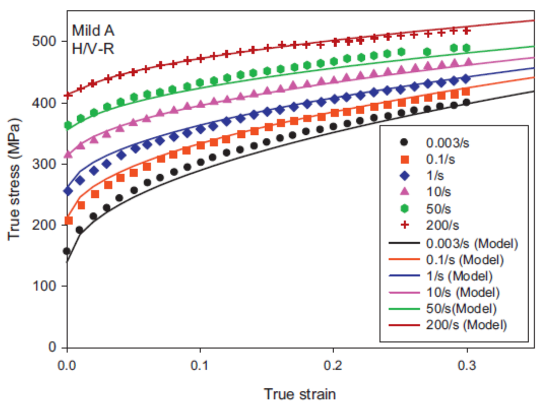

Figure 10. Stress x strain curves for a mild steel at several strain rates (Kim et al, 2012).

Considering the viscoplastic behavior thus leads to a model with a closer description of the reality. This was attempted here, and the related results are presented in this section.

Fig. 11 shows force vs. displacement curves for tests performed at α= 5º, the initial yield strength of 275MPa, friction coefficient of 0.1 to 4m/s speed, 1m/s and $1 \cdot 10^{-5}$m/s.

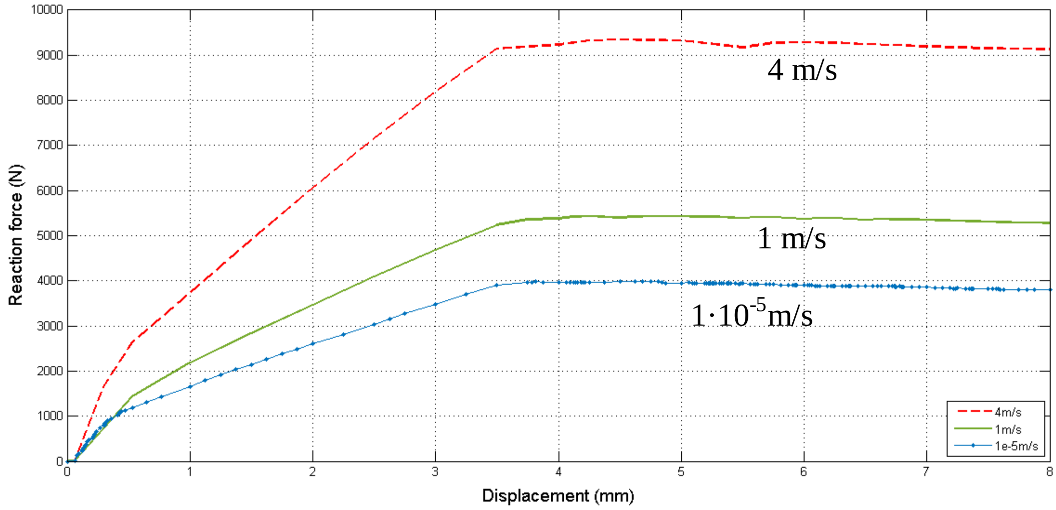

Figure 11. Force x displacement curves for different drawing speeds.

As a first result, Fig. 11 shows that there is an increase in the drawing force with increasing the drawing speed, as expected. Note that the comptuded increase is significant, more than doubling the drawing force compared to the quasi static simulations. It is also worth pointing out that the increase in the drawing force is nonlinearly proportional to the increase in the drawing speed.

Figure 12 shows the plastic strain rate of the wire during the reduction in quasi static conditions, at 1m/s and at 4m/s drawing speed.

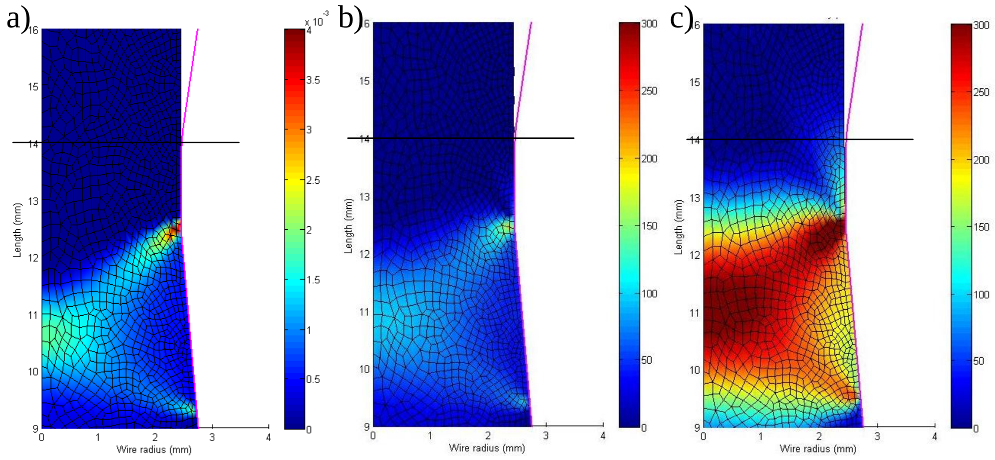

Figure 12. Plastic strain rate ($\dot{\kappa}$) s^{-1} for V= $1{\cdot}10^{-5}$ m/s (a), 1m/s (b) and 4m/s (c).

Figure 13 shows the distribution of von Mises stress (MPa) for α= 5º, V=$1{\cdot}10^{-5}$ m/s and 4m/s and the initial yield stress of 275 MPa.

The drawing speed significantly alters the values of stresses due to higher strain rates in the material. The von Mises stresses, for example, doubled at the speed of 4m/s compared to the quasi static case. Another interesting point is that residual stresses, while high, are distributed with a smaller inhomogeneity over the entire radius of the wire, ensuring a softer variation of the stresses in the simulations at 4m/s.

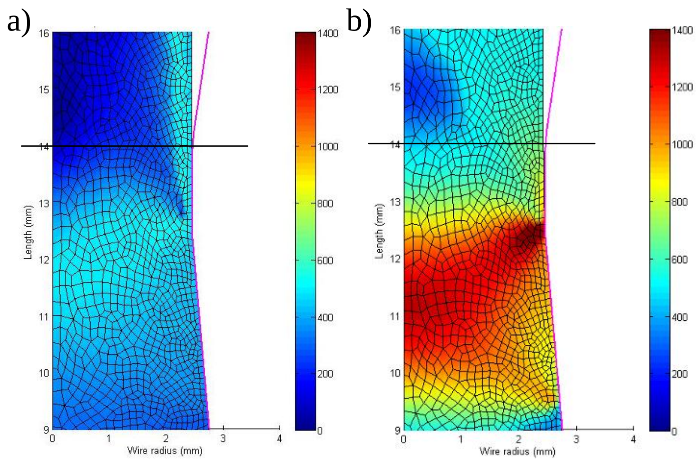

Figure 13. Distribution of von Mises stress (MPa) for V= 1·10^{-5} m/s (a) and 4m/s (b).

The deformations in all directions showed similar values. So the process speed is not a dominant factor for total strains, although it has a high influence on strain rates. Despite the high residual stress, the yield strength of the material after reduction, for all drawing speeds reached average value of 500MPa. Therefore, it can be stated that the strain rate influences the stresses during forming, but it causes no significant changes in the final product.

4 CONCLUSION

This research conducted a parametric study between various combinations of material and process parameters, the following conclusions can be drawn from this work:

• α is important in the stress distribution during and after the reduction process;

• Higher drawing speeds increase stresses and drawing force significantly but does not modify the end product;

• Increasing friction increases the drawing force;

• Frictional effects depend on the tool geometry;

• Dominant wire drawing parameters were observed to be:

- μ - undesirable in the process;
- Viscoplastic behavior raising stresses and drawing force with increasing the drawing speeds;
- α - the higher semi angle, the higher concentration of stresses;

The model used in this study has some limitations that could be lifted to approach better the actual process used in the industry. The variation of temperature during the drawing is a factor that was not considered in the simulations, since for a 10% reduction of the wire, and low semi angle, the temperature increase isn't high (around 20ºC), according to El-Domiaty and Kassab (1998). The viscoplastic exponent (n_{vp}) should correspond to a more realistic value (other than 1) and will be performed in future work. The coefficient of friction and viscosity were held constant for the tests, however, these parameters vary according to the strain rate and temperature, respectively. A more complex friction law can be included in the model in the future.

Acknowledgements

The first author is grateful to the Federal University of Ceará for the financial support and the Aço Cearense for their collaboration.

REFERENCES

Baek, H.M., Young, G.J., Sun, K.H., Yong-Taek, I., Il-Heon, S., Duk-Lak, L. 2012. Numerical study on the evolution of surface defects in wire drawing. *Journal of Materials Processing Technology,* vol. 212, pp. 776-785.

Belo, J.S. *Simulação do efeito da variação dos parâmetros de trefilação em aços aplicados à construção civil, através de elementos finitos*. 2014. Bachelor Thesis, Universidade Federal do Ceará/Fortaleza.

Bihamta, R., Bui, Q.H., Guillot, M., D'Amours, G., Rahem, A., Fafard, M. 2011. A new method for production of variable thickness aluminium tubes: Numerical and experimental studies. *Journal of Materials Processing Technology,* vol. 211, pp. 578-589.

Chevalier, L. 1992. Prediction of defects in metal forming: Application to wire drawing. *Journal of Materials Processing Technology*. vol. 32, pp. 145-153.

Celentano, D.J., Palacios, M.A., Rojas, E.L., Cruchaga, M.A., Artigas, A.A., Monsalve, A.E. 2009. Simulation and experimental validation of multiple-step wire drawing processes. *Finite Elements in Analysis and Design*. vol. 45, pp. 163-180.

Chin, R.K., Steif, P.S. 1995. A Computational study of strain inhomogeneity in wire drawing. *International Journal of Machine Tools and Manufacture*. vol. 35, n. 8, pp. 1087-1098.

Cristecu, N. 1980. On the optimum die angle in fast wire drawing. *Journal of Mechanical Working Technology*. vol. 3, pp. 275-287.

El-Domiaty, A., Kassab, S.Z. 1998. Temperature rise in wire-drawing. *Journal of Materials Processing Technology*. vol. 83, pp. 72-83.

Felder, E., Levrau, C., Mantel, M., Dinh, N.G.T. 2012. Identification of the work of plastic deformation and the friction shear stress in wire drawing. *Wear*. vol. 286-287, pp. 27-34.

Filice, L., Ambrogio, G. Guerriero, F. 2013. A multi-objective approach for wire-drawing process. Procedia CIRP. *8th CIRP Conference on Intelligent Computation in Manufacturing Engineering.* vol. 12, pp. 294-299.

Haddi, A., Imad, A., Vega, G. 2011. Analysis of temperature and speed effects on the drawing stress for improving the wire drawing process. *Materials and Design*. vol.12, pp. 4310-4315.

Heegaard, J.-H. & Curnier, A. 1993. *An augmented Lagrangian method for discrete large-slip contact problems Int. J.* Numer. Methods Eng., John Wiley and Sons Ltd., 36, 569-593.

Huh, J., Huh, H., Lee, C.S. 2013. Effect of strain rate on plastic anisotropy of advanced high strength steel sheets. *International Journal of Plasticity*. vol. 44, pp. 23-46.

Kim, T.H., Kim, B.M., Choi, J.C. 1997. Prediction of die wear in the wire-drawing process. *Journal of Materials Processing and Technology*. vol. 65, pp. 11-17.

Magalhães, F.C., Pertence, A.E.M., Campos, H.B., Aguilar, M.T.P, Cetlin, P.R. 2012. Defects in axisymmetrically drawn bars caused by longitudinal superficial imperfections in the initial material. *Journal of Materials Processing and Technology*. vol. 212, pp. 237-248.

Pietrzak, G. & Curnier, A. 1999. Large deformation frictional contact mechanics: continuum formulation and augmented Lagrangian treatment. *Comp. Meth. Appl. Mech. Eng.*, Elsevier Science S.A., vol. 177, pp. 351-381.

Ponthot, J. 2002. *Unified stress update algorithms for the numerical simulation of large deformation elasto-plastic and elasto-viscoplastic processes Int. J*. Plas., vol. 18, pp. 91-126.

Toribio, J., Lorenzo, M., Vergara, D., Kharin, V. 2014. Influence of the die geometry on the hydrogen embrittlement susceptibility of cold drawn wires. *Engineering Failure Analysis*. vol. 36, pp. 215-225.

Toribio, J., Lorenzo, M., Vergara. 2015. On the use of varying die angle for improving the resistance to hydrogen embrittlement of cold drawn prestressing steel wires. *Engineering Failure Analysis*. vol. 45, pp. 273-282.